

Nanoscale Confinement Effects on Ionic Conductivity of Solid Polymer Electrolytes: The Interplay between Diffusion and Dissociation

Xiupeng Chen[†] and Xian Kong^{*,†,‡}

[†]*South China Advanced Institute for Soft Matter Science and Technology, School of Emergent Soft Matter, South China University of Technology, Guangzhou 510640, China*
[‡]*Guangdong Provincial Key Laboratory of Functional and Intelligent Hybrid Materials and Devices, South China University of Technology, Guangzhou 510640, China*

E-mail: xk@scut.edu.cn

Abstract

Solid polymer electrolytes (SPEs) are attractive for next-generation lithium metal batteries but still suffer from low ionic conductivity. Nanostructured materials offer design concepts for SPEs with better performance. Using molecular dynamics simulation, we examine SPEs under nanoscale confinement, which has been demonstrated to accelerate the transport of neutral molecules such as water. Our results show that while ion diffusion indeed accelerates by more than two orders of magnitude as the channel diameter decreases from 15 nm to 2 nm, the ionic conductivity does not increase significantly in parallel. Instead, the ionic conductivity shows a non-monotonic variation, with an optimal value above, but on the same order as, its bulk counterparts. This trend is due to enhanced ion association with decreasing channel size, which reduces the number of effective charge carriers. This effect competes with accelerated ion diffusion, leading to the non-monotonicity in ion conductivity.

Keywords: solid polymer electrolytes, nanoconfinement, ionic conductivity, ion correlation, molecular dynamics simulation

The next-generation Li-based batteries¹ involve the usage of lithium metal anode paired with high-voltage cathodes such as sulfur² or air.³ However commercialization of such batteries has been plagued by instability during charge/discharge cycling that is rooted in the intrinsic incompatibility between lithium metal anode and liquid electrolytes, which are developed for current lithium-ion batteries.⁴ Solid-state electrolytes are expected to be able to mitigate the instability and therefore enabling Li-metal batteries.⁵ Solid-state electrolytes can be divided into two categories: inorganic ceramic electrolytes and solid polymer electrolytes, each with its own advantages and disadvantages.^{5,6}

Solid polymer electrolytes (SPEs) are basically lithium-salt-doped polymers.⁷ The most well-known SPEs are based on poly(ethylene oxide) (PEO), which was discovered over half a century ago.⁸ They remain the first candidate for SPEs. SPEs have many merits compared with ceramic or traditional liquid electrolytes including ease of processability, low flammability and toxicity, interfacial compatibility at the electrode surface, and moderate mechanical stiffness for Li dendrites suppression. The lethal weaknesses of SPEs^{9,10} that prevent them from being deployed in the commercial battery are low ionic conductivity and low Li⁺ transference number, that is, the fraction of current carried by Li⁺ movement.

A lingering dilemma in improving the conductivity of SPEs is that increased conductivity usually brings about compromised mechanical stiffness.⁹ For example, operating at high temperatures,¹¹ using lower molecular weight PEO chains¹² or adding plasticizer¹³ can improve the ion conductivity of SPEs, but reduce mechanical strength. In recent years, a number of approaches have been attempted to enhance the conductivity of SPEs, while maintaining the stiffness. These strategies include designing new non-PEO polymers,^{14–18} turning to block copolymers that combine one block for ion conductivity and another block for mechanical strength,¹⁹ introducing nano-fillers,²⁰ designing polymer/inorganic composite electrolytes^{1,21} etc. Despite partial successes in optimizing SPEs performance, these meth-

ods are still far from meeting the requirements for practical batteries. Therefore, new design concepts are still necessary for further improving SPEs performance.

The emergence of various nanomaterials provides efficient solutions to technical issues in various fields. For example, the enrollment of carbon nanomaterials as anode materials allows stable recycling of lithium metal anode.^{22,23} With these successes, it becomes interesting to see if we can leverage on the features of those nanomaterials to improve the performance of SPEs. It has long been known that mass transport inside nano-confined space differs significantly from its bulk counterpart. For example, water can diffuse rapidly inside carbon nanotubes, with a flow rate that is several orders higher than in macroscopic pipes.²⁴⁻³⁰

Several experimental studies already observed extremely fast ion transport in SPEs confined in nanochannels.³¹ For example, Zhang et al prepared anodized aluminum oxide (AAO) and polymer composite electrolytes by infiltrating melted PEO electrolytes into the vertically aligned pores of AAO.³² The SPEs confined in AAO pores show a conductivity that is an order of magnitude higher than bulk SPE at room temperature. Another benefit of this design is that the ionic conductivity and mechanical strength of the composite electrolytes are not coupled to each other any longer. Therefore, it is possible to use short PEO chains to further enhance ionic conductivity without sacrificing rigidity, permitting more versatile design choices. Similarly, PEO-based SPEs confined inside organic nanoporous matrix such as polyimide film also show an increased ionic conductivity that is more than 4 times the ionic conductivity of bare SPEs.³³ Nevertheless, the enhanced ionic conductivity of these two composite SPEs results from factors that are not directly related to nanoconfinement. For the SPEs confined in AAO channels, a lower degree of crystallization of PEO underpins the fast ion transport. Whereas for the SPEs confined in pores within polyimide film matrix, the alignment of the PEO chains was thought to be the cause. Therefore, it remains to be seen if nanoscale confinement alone can enhance ionic conductivity and if so, to what extent.

Here, we design a molecular dynamics simulation study to answer these questions. We conduct MD simulations of SPEs in inert nanochannels with diameters smaller than 15 nm.

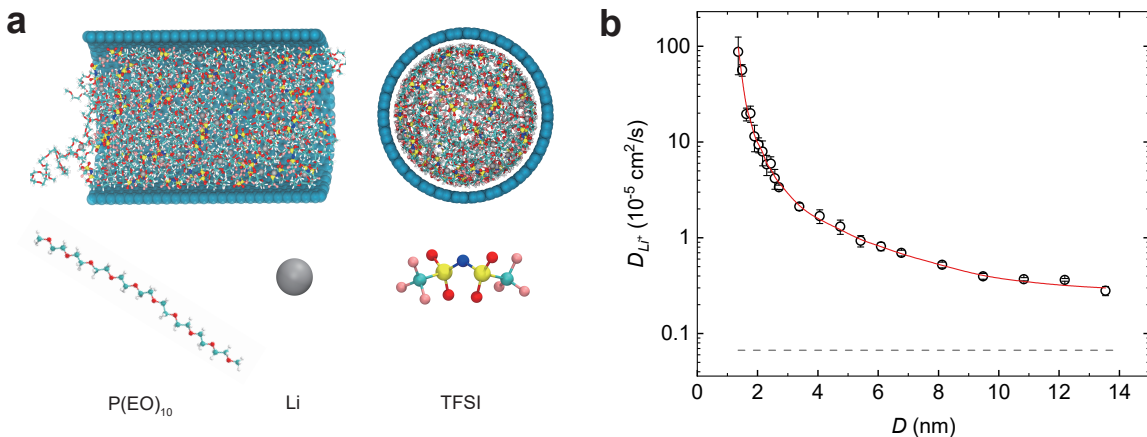


Figure 1: Solid polymer electrolyte (SPE) confined in a nanochannel. (a) Snapshots of a typical simulation system. Color code: gray, lithium; red, oxygen; blue, nitrogen; yellow, sulfur; cyan, carbon; pink, fluoride; white, hydrogen. (b) Diffusion coefficients of lithium-ion (D_{Li^+}) versus the diameter of nanochannel (D). The gray dashed line is the diffusion coefficient of Li^+ in the bulk electrolyte. The red line is a guide to the eye.

(Fig. 1) We find that ions show a fast diffusion rate that is orders of magnitude higher than bulk SPEs. Nevertheless, ionic conduction does not show a comparable acceleration in nanochannels accordingly. In large nanochannels (for example channel diameter larger than 10 nm), SPE conductivity is only slightly higher than its bulk counterpart. As the channel size decreases, the conductivity increases slowly, attaining a maximum when the channel diameter is about 6 nm. However, the optimal conductivity is on the same order as the bulk conductivity. Further decreasing the channel size leads to abrupt deterioration of ionic conductivity. The reason for this trend is that nano-confinement enhances ion correlations, leaving less dissociated ions or charged ion clusters as charge carriers. The competition between decreased ion dissociation and increased ion diffusion leads to the non-monotonic change of ion conductivity with decreasing channel size. These findings manifest the intricacy of ionic transport behavior that is in sharp contrast with single-component transport like water, and the necessity of finely tuning the nanostructure to effectively improve the SPE conductivity.

A typical simulation system comprises a cylindrical nanochannel filled with typical SPE of LiTFSI/PEO electrolytes (Fig. 1a). Unless otherwise stated, the PEO chains have a

length of 10 monomers. This short chain length is to enable fast dynamics so that the MD sampling can be sufficient within reasonable computational cost. A high temperature of 363 K was used for all simulations. This high temperature not only accelerates system dynamics, but also excludes any interference with PEO crystallization,³⁴ which occurs below 333 K.³⁵ The salt amount is quantified by the number of Li⁺ to that of EO monomers, $r = [\text{Li}^+]/[\text{EO}]$, and is kept constant at $r = 0.1$ for all simulations.

Fig. 1b presents the diffusion coefficients of Li⁺ (D_{Li^+}) in nanochannels of different diameters (D). Obviously, ion diffusion in nanochannel is faster than its bulk counterpart. Even in the largest channel studied ($D=13.541$ nm), the ion diffusion coefficient is about an order higher than in bulk. The degree of acceleration depends on the channel size and is more prominent with a smaller channel size. The diffusion coefficient increases by more than 2 orders when the nanochannel radius decreases from 6.771 nm to 0.678 nm. Increased diffusion coefficient of water in nanotubes has also been reported,^{28,36,37} reflecting the universality of diffusion acceleration induced by nanoscale confinement.

To gain more insights into the effects of nanoconfinement, we accumulated the density profiles of different components in the nanochannel (Fig. 2). All 2D density profiles of Li⁺ in the perpendicular plane of the channel show circular symmetry, mirroring the cylindrical symmetry of the nanochannel. Close to the channel wall, Li⁺ shows obvious layering, demonstrating the perturbation of the confinement. After about 3 oscillations, the density plateaus to the bulk value in the center of the channel. From the 1D density profiles along the radial direction (Fig. 2d), we can see that the channel diameter barely affects the ion layering behavior when $D \geq 4.063$ nm. That is, neither the height nor the period of the density oscillation changes as D varies. When $D < 4.063$ nm, the channel size is comparable to the thickness of the perturbed layer. Further decreasing the diameter of the channel greatly changes the density profiles, in terms of both the number of peaks and peak amplitude. For example, the number of peaks will decrease from 3 to 2 ($D = 2.709$ nm). The height of the first peak from the wall also increases, indicating a stronger layering. Note

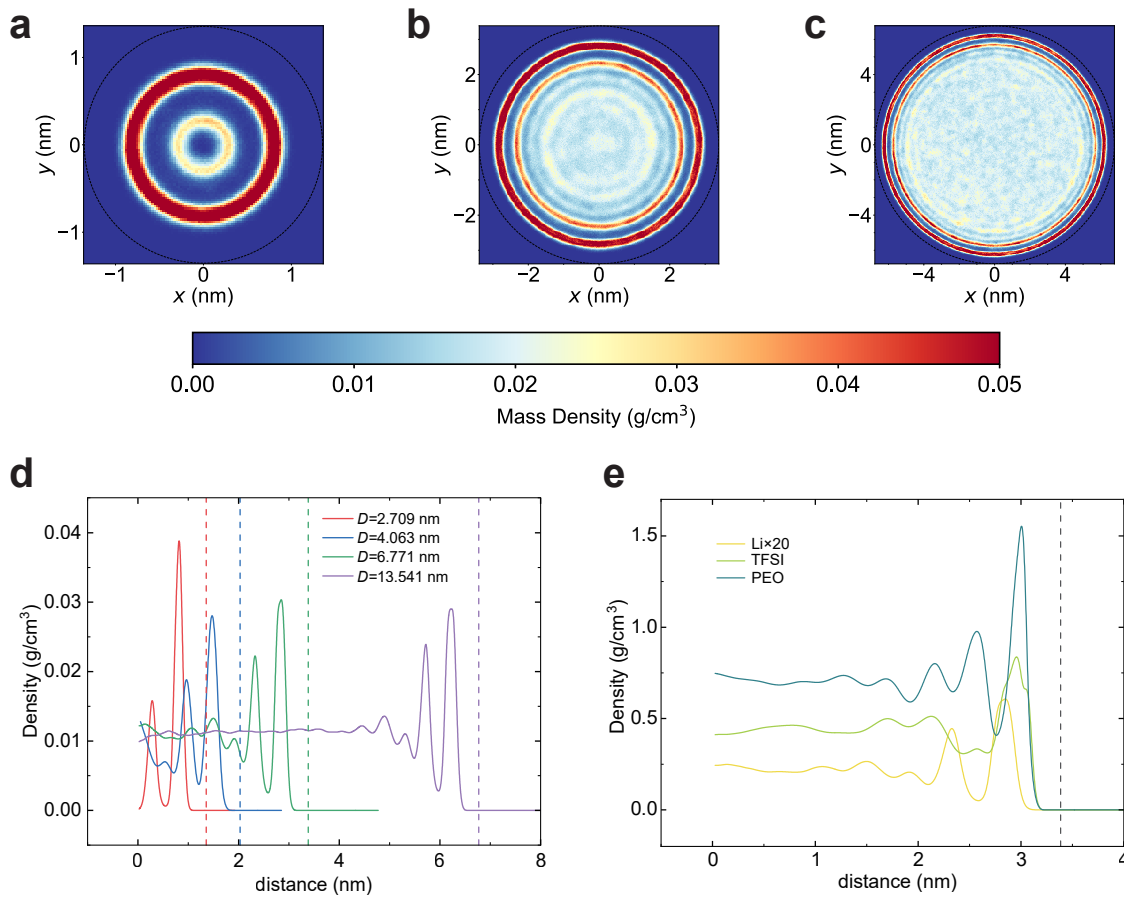


Figure 2: Density distributions inside nanochannel. (a-c) 2-dimensional mass density profiles of Li^+ in channels with diameters of 2.704 nm (a), 6.771 nm (b), and 13.541 nm (c). The black dashed line in each figure is the position of the channel wall. (d) Radial mass density profiles of Li^+ in four representative channels. The dashed lines are the location of the channel walls. (e) Radial mass density profiles of Li^+ , TFSI and PEO in the channel with a diameter of 6.771 nm.

that when $D < 4.063 \text{ nm}$, D_{Li^+} increases more rapidly with the decrease of D than when $D > 4.063 \text{ nm}$. This manifests the role of confinement in improving ion diffusion.

Comparing the density profiles of different components in the confined SPE (Fig. 2e), we find that the oscillation of Li^+ density profile is out of phase with that of PEO, while TFSI is in phase with PEO. The first peak of PEO and TFSI is closer to the channel wall than the first peak of Li^+ . As will be shown in next section, the solvation of Li^+ is very strong, and the neutral channel wall cannot drive the desolvation of Li^+ .

Though accelerated ion diffusion is beneficial for electrochemical device operation, it

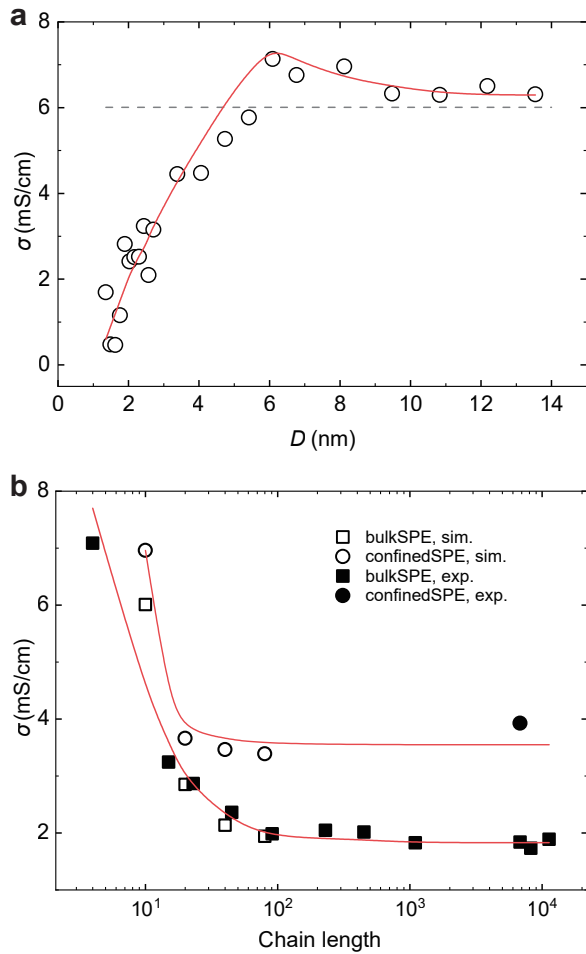


Figure 3: (a) The conductivity of electrolytes (σ) versus the diameter of the channel (D). The gray dashed line is the ionic conductivity of bulk SPE. (b) The dependence of conductivity on chain length from this work and from experiments. The diameter of confining nanochannel is 6.771 nm. The experimental values are measured at 363 K.^{12,32} Red lines are guides to the eye. Error bars are about the same size as markers, so not shown.

does not guarantee improved performance. Another (more) important quantity is the ionic conductivity (σ), which is related to the electrochemical resistance of SPE. We calculated the conductivity of confined electrolytes based on Onsager transport coefficients,^{38–40} which were extracted from molecular dynamics trajectories according to Green–Kubo relations^{41–43} (see simulation methods in SI Section 1). Fig. 3a shows the conductivity (σ) of SPEs in nanochannels of different diameters (D).

In the high D regime, σ approaches the expected bulk conductivity limit. For $D < \sim 5$ nm, there is a steep decline in σ , indicating that overly strong confinement dampens ionic charge

transport. At moderate D values around 6 to 8 nm, σ slightly surpasses the bulk conductivity, demonstrating that the nanoscale confinement effect alone (independently of crystallinity or chain alignment) can enhance SPE conductivity. As a result, the conductivity of confined SPEs exhibits a non-monotonic trend as the diameter of the confining nanochannel decreases from 14 to 2 nm.

To provide further evidence that nanoscale confinement can enhance conductivity in SPEs, we conducted additional simulations using longer PEO chains consisting of 20, 40, and 80 monomers under both bulk and confined conditions (Fig. 3b). When the chain length is small, σ depends on the chain length significantly. Increasing chain length leads to a decrease in conductivity due to the apparent slowdown of polymer segmental motions for both bulk and confined SPEs. Further increase in PEO chain length only brings a slow decay in σ toward a plateau, consistent with previous simulation studies on bulk SPE.⁴⁴ Note that our simulated conductivity agrees well with experimental results measured at temperatures around 363 K,^{12,32} across more than four orders of chain length. This is probably because that the force field we used was specially optimized to reproduce experimental ion diffusion behavior.⁴⁵

A noteworthy finding in Fig. 3b is that all confined SPEs, no matter what the PEO molecular weight is, have higher σ than corresponding bulk SPEs with the same chain length. This demonstrates that the nano-confinement-enhanced conductivity persists in all SPEs with PEO of different molecular weights. What's more, the enhancement is more pronounced for SPEs with long PEO chains, as the plateau value of the bulk conductivity is low. The critical molecular weight for entanglement of PEO chains is 2 kg/mol, or equivalently a chain length of 45.⁴⁶ Above the critical entanglement chain length, the ionic conductivity is not sensitive to chain length.¹² Therefore, our results imply strongly that nanoscale confinement can improve ionic conductivity in real SPEs.

From the discussions above, we can summarize that the confinement channel can indeed enhance ion conductivity, but this enhancement requires an optimum channel size. A too-

small channel gives no conductivity enhancement but significantly decreases the conductivity instead. This is not expected based only on the ion diffusion behavior, which accelerates with decreasing channel size. Examination of end-to-end distance distribution of PEO chains reveals that PEO chain conformation only show deviations from bulk chain behavior in nanochannels with $D \leq 2.709$ nm (Fig. S3). This suggests that the decrease in conductivity has no relation with the change in chain conformation due to confinement.

The motion of net charges underpins ionic conductivity. Ionic conductivity is determined by not only how fast ions move, but also how many effectively charged ions there are in the electrolytes. In other words, ionic conductivity hinges on the correlations among ions,^{42,47} and depends highly on the degree of ion dissociation. Ions can exist in various identities,⁴⁸ including isolated ions (or dissociated ions), contact ion pairs (CIPs), solvent-separated ion pairs (SSIPs), or ion clusters. Ignoring the contributions to σ from charged clusters,⁴⁹ ionic conductivity can be estimated by,⁵⁰

$$\sigma = ec\xi(\mu_+ + \mu_-), \quad (1)$$

where e is the unit charge, c is the ion number density, and ξ is the effective degree of ion dissociation, $\xi = [\text{free ions}] / [\text{total ions}]$. μ_i is the mobility of species i , which is usually proportional to its diffusivity according to Einstein relation,⁵¹ $D_i = k_B T \mu_i / e$. As shown above, a smaller channel diameter gives a higher ion diffusivity, (hence higher ion mobility), which is favorable for increasing conductivity.

The inferior ionic conductivity in highly confined nanochannel is plagued by the enriched ion association therein. In other words, confinement drives more ion association, resulting in a smaller degree of ion dissociation ξ , which brings down ion conductivity according to eq. 1. Fig. S4 presents the effective dissociation ξ obtained from eq. 1. As expected, ξ is significantly lower for SPEs confined in nanochannels than bulk SPE, and decreases as channel diameter (D) decreases.

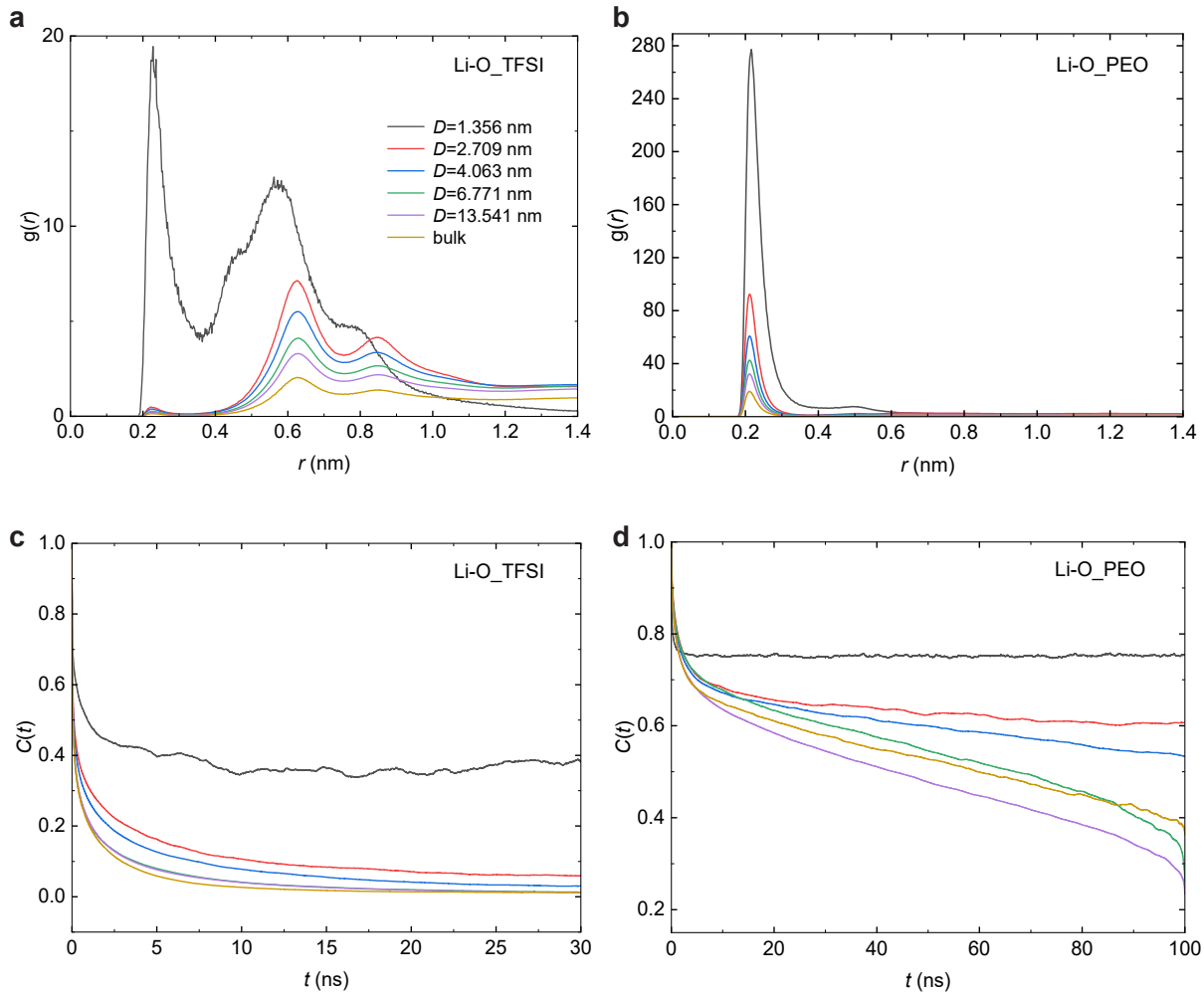


Figure 4: Correlations among different components of SPE. (a-b) Radial distribution functions, $g(r)$, between Li^+ and oxygen atoms in TFSI(a) and PEO(b). (c-d) Residence time distribution, $C(t)$, of TFSI(c) and PEO(d) around Li^+ .

To illustrate this in more detail, we calculated the radial distribution function $g(r)$ and residence time correlation function $C(t)$ between Li^+ and anion or PEO (Fig. 4). While $g(r)$ reflects spacial and static correlations, $C(t)$ reflects temporal and dynamic correlations.⁵² Fig. 4a shows $g(r)$ between Li^+ and oxygen atoms of TFSI, for SPEs in representative nanochannels, as well as in the bulk state. All confined SPEs except for the one in $R = 0.678$ nm show similar $g(r)$ as bulk SPEs, with a minor first peak and major second and third peaks. The first peak is weak because in PEO electrolytes, Li^+ is more likely to bind with PEO, as validated by the sharp first peak in the $g(r)$ between Li^+ and oxygen from PEO

(Fig. 4b). This also means the ion pairs mostly exist in the form of solvent-separated ion pairs (SSIPs), instead of contact ion pairs (CIPs). This agrees with experimental findings^{53,54} and previous simulation results.^{55,56}

As the channel size decreases, the peaks in $g(r)$ between Li^+ and TFSI become more pronounced, implying a stronger correlation between Li^+ and anion. In the smallest channel examined ($D = 1.356 \text{ nm}$), not only does the height of the $g(r)$ peaks increases, the shape also transforms into one showing a dominant first peak, indicating the ion pairs are becoming CIPs. This means that high-degree confinement can change both the degree of correlation and the nature of correlations in SPEs. Similarly, the peak in $g(r)$ between Li^+ and oxygen from PEO also increases as the channel shrinks (Fig. 4b). This means all inter-molecular correlations are enhanced concurrently as the confinement effect strengthens.

The dynamical or temporal correlations, quantified by $C(t)$, show a trend that is compatible with $g(r)$ (Fig. 4c). In nanochannels, $C(t)$ between Li^+ and TFSI decays more slowly than in bulk SPE. This means the cation and anion are prone to stay with each other and consequently move together for a longer period, which contributes essentially none to conductivity. The decay slows down as nanochannel diameter decreases, supporting the above findings that confinement enhances cation-anion correlation. Likewise, $C(t)$ between Li^+ and PEO show similar behavior (Fig. 4d). In the smallest channel examined ($D = 1.356 \text{ nm}$), the decay in $C(t)$ between Li^+ and PEO is so slow that it even flattens, signifying that some Li^+ 's bind with the same set of PEO segments throughout the simulation.

The inert nanochannel wall provides no strong solvation to Li^+ as implied by the distal first peak of Li^+ from nanochannel wall (Fig. 2e). This weak solvation environment promotes the binding between Li^+ and anions, resulting in less ionic dissociation. The deterioration of ionic conductivity due to enhanced ion correlation has also been reported in polymers with low dielectric constant,⁵⁷ suggesting its universality. This effect competes with the confinement-induced diffusion acceleration, leading to the non-monotonic dependence of ionic conductivity on channel size.

In conclusion, we examined the effects of nanoconfinement on a typical solid polymer electrolyte (SPE) based on LiTFSI/PEO. SPEs confined in nanoscale channels show accelerated ion diffusion compared to bulk SPEs. The ion diffusion coefficient increases by more than two orders as the channel diameter decreases from 15 nm to 2 nm. However, the ionic conductivity does not show paralleling enhancement. This is because ion conductivity depends not only on how fast ions diffuse but also on the effective net charges. Nanoconfinement drives more ion association, giving less dissociated ions with smaller channel diameters. This effect competes with the accelerated ion diffusion, leading to a non-monotonic dependence of ion conductivity on channel size. These findings demonstrate that the ion transport behavior is more sophisticated than the transport of neutral solvents (eg. water) in nanochannels, and also provide indispensable implications for designing nano-structured materials for composite solid polymer electrolytes. An intriguing avenue for future research is to explore the potential benefits of surface modification of the nanochannel. For instance, grafting Lewis acidic sites or introducing local polarity might improve the solvation ability of the nanochannel towards Li^+ , thereby facilitating ionic dissociation and potentially enhancing ionic conductivity.

Acknowledgement

This research has been supported by Guangdong Basic and Applied Basic Research Foundation (2022A1515110016), the Recruitment Program of Guangdong (2016ZT06C322) and TCL Science and Technology Innovation Fund.

Supporting Information Available

The following files are available free of charge: simulation and analysis methods, effects of packing density on ionic conductivity, details on the preparation of simulation systems, system parameters and compositions, polymer chain end-to-end distance distribution, effective dissociation ratio.

References

- (1) Wang, Y.; Zanelotti, C. J.; Wang, X.; Kerr, R.; Jin, L.; Kan, W. H.; Dingemans, T. J.; Forsyth, M.; Madsen, L. A. Solid-state rigid-rod polymer composite electrolytes with nanocrystalline lithium ion pathways. *Nature Materials* **2021**, *20*, 1255–1263.
- (2) Bruce, P. G.; Freunberger, S. A.; Hardwick, L. J.; Tarascon, J.-M. Li–O₂ and Li–S batteries with high energy storage. *Nature Materials* **2012**, *11*, 19–29.
- (3) Lu, J.; Jung Lee, Y.; Luo, X.; Chun Lau, K.; Asadi, M.; Wang, H.-H.; Brombosz, S.; Wen, J.; Zhai, D.; Chen, Z., et al. A lithium–oxygen battery based on lithium superoxide. *Nature* **2016**, *529*, 377–382.
- (4) Lin, D.; Liu, Y.; Cui, Y. Reviving the lithium metal anode for high-energy batteries. *Nature Nanotechnology* **2017**, *12*, 194–206.
- (5) Manthiram, A.; Yu, X.; Wang, S. Lithium battery chemistries enabled by solid-state electrolytes. *Nature Reviews Materials* **2017**, *2*, 1–16.
- (6) Kim, S.; Kim, J.-S.; Miara, L.; Wang, Y.; Jung, S.-K.; Park, S. Y.; Song, Z.; Kim, H.; Badding, M.; Chang, J., et al. High-energy and durable lithium metal batteries using garnet-type solid electrolytes with tailored lithium-metal compatibility. *Nature Communications* **2022**, *13*, 1–12.
- (7) Xue, Z.; He, D.; Xie, X. Poly(ethylene oxide)-based electrolytes for lithium-ion batteries. *J. Mater. Chem. A* **2015**, *3*, 19218–19253.
- (8) Fenton, D. E.; Parker, J. M.; Wright, P. V. Complexes of alkali metal ions with poly(ethylene oxide). *Polymer* **1973**, *14*, 589.
- (9) Long, L.; Wang, S.; Xiao, M.; Meng, Y. Polymer electrolytes for lithium polymer batteries. *Journal of Materials Chemistry A* **2016**, *4*, 10038–10069.

- (10) Bocharova, V.; Sokolov, A. P. Perspectives for Polymer Electrolytes: A View from Fundamentals of Ionic Conductivity. *Macromolecules* **2020**, *53*, 4141–4157.
- (11) Steele, B.; Lagos, G.; Spurdens, P.; Forsyth, C.; Foord, A. Behaviour of Li_xV₆O₁₃ and Li_xTiS₂ composite electrodes incorporating polyethylene oxide based electrolytes. *Solid State Ionics* **1983**, *9-10*, 391–398.
- (12) Teran, A. A.; Tang, M. H.; Mullin, S. A.; Balsara, N. P. Effect of molecular weight on conductivity of polymer electrolytes. *Solid State Ionics* **2011**, *203*, 18–21.
- (13) Bandara, L.; Dissanayake, M.; Mellander, B.-E. Ionic conductivity of plasticized (PEO)-LiCF₃SO₃ electrolytes. *Electrochimica acta* **1998**, *43*, 1447–1451.
- (14) Zhang, J.; Zhao, J.; Yue, L.; Wang, Q.; Chai, J.; Liu, Z.; Zhou, X.; Li, H.; Guo, Y.; Cui, G., et al. Safety-reinforced poly (propylene carbonate)-based All-solid-state polymer electrolyte for ambient-temperature solid polymer lithium batteries. *Advanced Energy Materials* **2015**, *5*, 1501082.
- (15) Jones, S. D.; Nguyen, H.; Richardson, P. M.; Chen, Y.-Q.; Wyckoff, K. E.; Hawker, C. J.; Clément, R. J.; Fredrickson, G. H.; Segalman, R. A. Design of polymeric zwitterionic solid electrolytes with superionic lithium transport. *ACS Central Science* **2022**, *8*, 169–175.
- (16) Chen, F.; Wang, X.; Armand, M.; Forsyth, M. Cationic polymer-in-salt electrolytes for fast metal ion conduction and solid-state battery applications. *Nature Materials* **2022**, *21*, 1175–1182.
- (17) Mindemark, J.; Lacey, M. J.; Bowden, T.; Brandell, D. Beyond PEO—Alternative host materials for Li⁺-conducting solid polymer electrolytes. *Progress in Polymer Science* **2018**, *81*, 114–143.

- (18) Savoie, B. M.; Webb, M. A.; Miller III, T. F. Enhancing cation diffusion and suppressing anion diffusion via Lewis-acidic polymer electrolytes. *The journal of physical chemistry letters* **2017**, *8*, 641–646.
- (19) Bouchet, R.; Maria, S.; Meziane, R.; Aboulaich, A.; Lienafa, L.; Bonnet, J.-P.; Phan, T. N.; Bertin, D.; Gigmes, D.; Devaux, D., et al. Single-ion BAB triblock copolymers as highly efficient electrolytes for lithium-metal batteries. *Nature materials* **2013**, *12*, 452–457.
- (20) Tang, C.; Hackenberg, K.; Fu, Q.; Ajayan, P. M.; Ardebili, H. High ion conducting polymer nanocomposite electrolytes using hybrid nanofillers. *Nano letters* **2012**, *12*, 1152–1156.
- (21) Liu, W.; Lee, S. W.; Lin, D.; Shi, F.; Wang, S.; Sendek, A. D.; Cui, Y. Enhancing ionic conductivity in composite polymer electrolytes with well-aligned ceramic nanowires. *Nature energy* **2017**, *2*, 1–7.
- (22) Zheng, G.; Lee, S. W.; Liang, Z.; Lee, H.-W.; Yan, K.; Yao, H.; Wang, H.; Li, W.; Chu, S.; Cui, Y. Interconnected hollow carbon nanospheres for stable lithium metal anodes. *Nature nanotechnology* **2014**, *9*, 618—623.
- (23) Lin, D.; Liu, Y.; Liang, Z.; Lee, H.-W.; Sun, J.; Wang, H.; Yan, K.; Xie, J.; Cui, Y. Layered reduced graphene oxide with nanoscale interlayer gaps as a stable host for lithium metal anodes. *Nature Nanotechnology* **2016**, *11*, 626—632.
- (24) Secchi, E.; Marbach, S.; Niguès, A.; Stein, D.; Siria, A.; Bocquet, L. Massive radius-dependent flow slippage in carbon nanotubes. *Nature* **2016**, *537*, 210–213.
- (25) Hummer, G.; Rasaiah, J. C.; Noworyta, J. P. Water conduction through the hydrophobic channel of a carbon nanotube. *Nature* **2001**, *414*, 188–190.

- (26) Joseph, S.; Aluru, N. Why are carbon nanotubes fast transporters of water? *Nano letters* **2008**, *8*, 452–458.
- (27) Alexiadis, A.; Kassinos, S. Molecular simulation of water in carbon nanotubes. *Chemical reviews* **2008**, *108*, 5014–5034.
- (28) Striolo, A. The mechanism of water diffusion in narrow carbon nanotubes. *Nano letters* **2006**, *6*, 633–639.
- (29) Walther, J. H.; Ritos, K.; Cruz-Chu, E. R.; Megaridis, C. M.; Koumoutsakos, P. Barriers to superfast water transport in carbon nanotube membranes. *Nano letters* **2013**, *13*, 1910–1914.
- (30) Nazari, M.; Davoodabadi, A.; Huang, D.; Luo, T.; Ghasemi, H. Transport phenomena in nano/molecular confinements. *ACS nano* **2020**, *14*, 16348–16391.
- (31) Meng, Y. S.; Srinivasan, V.; Xu, K. Designing better electrolytes. *Science* **2022**, *378*, eabq3750.
- (32) Zhang, X.; Xie, J.; Shi, F.; Lin, D.; Liu, Y.; Liu, W.; Pei, A.; Gong, Y.; Wang, H.; Liu, K.; Xiang, Y.; Cui, Y. Vertically Aligned and Continuous Nanoscale Ceramic–Polymer Interfaces in Composite Solid Polymer Electrolytes for Enhanced Ionic Conductivity. *Nano Letters* **2018**, *18*, 3829–3838, PMID: 29727578.
- (33) Wan, J. et al. Ultrathin, flexible, solid polymer composite electrolyte enabled with aligned nanoporous host for lithium batteries. *Nature Nanotechnology* **2019**, *14*, 705–711.
- (34) Borodin, O.; Smith, G. D. Mechanism of ion transport in amorphous poly (ethylene oxide)/LiTFSI from molecular dynamics simulations. *Macromolecules* **2006**, *39*, 1620–1629.

- (35) Croce, F.; Appeteccchi, G. B.; Persi, L.; Scrosati, B. Nanocomposite polymer electrolytes for lithium batteries. *Nature* **1998**, *394*, 456–458.
- (36) Thomas, J. A.; McGaughey, A. J. Reassessing fast water transport through carbon nanotubes. *Nano letters* **2008**, *8*, 2788–2793.
- (37) Jakobtorweihen, S.; Verbeek, M. G.; Lowe, C. P.; Keil, F. J.; Smit, B. Understanding the Loading Dependence of Self-Diffusion in Carbon Nanotubes. *Phys. Rev. Lett.* **2005**, *95*, 044501.
- (38) Onsager, L. THEORIES AND PROBLEMS OF LIQUID DIFFUSION. *Annals of the New York Academy of Sciences* **1945**, *46*, 241–265.
- (39) Fong, K. D.; Bergstrom, H. K.; McCloskey, B. D.; Mandadapu, K. K. Transport phenomena in electrolyte solutions: Nonequilibrium thermodynamics and statistical mechanics. *AIChE Journal* **2020**, *66*, e17091.
- (40) Vargas-Barbosa, N. M.; Roling, B. Dynamic ion correlations in solid and liquid electrolytes: how do they affect charge and mass transport? *ChemElectroChem* **2020**, *7*, 367–385.
- (41) Fong, K. D.; Self, J.; McCloskey, B. D.; Persson, K. A. Onsager Transport Coefficients and Transference Numbers in Polyelectrolyte Solutions and Polymerized Ionic Liquids. *Macromolecules* **2020**, *53*, 9503–9512.
- (42) Fong, K. D.; Self, J.; McCloskey, B. D.; Persson, K. A. Ion Correlations and Their Impact on Transport in Polymer-Based Electrolytes. *Macromolecules* **2021**, *54*, 2575–2591.
- (43) Zhang, Z.; Wheatle, B. K.; Krajniak, J.; Keith, J. R.; Ganesan, V. Ion mobilities, transference numbers, and inverse Haven ratios of polymeric ionic liquids. *ACS Macro Letters* **2019**, *9*, 84–89.

- (44) Brooks, D. J.; Merinov, B. V.; Goddard, W. A. I.; Kozinsky, B.; Mailoa, J. Atomistic Description of Ionic Diffusion in PEO–LiTFSI: Effect of Temperature, Molecular Weight, and Ionic Concentration. *Macromolecules* **2018**, *51*, 8987–8995.
- (45) Fang, C.-E.; Tsai, Y.-C.; Scheurer, C.; Chiu, C.-C. Revised Atomic Charges for OPLS Force Field Model of Poly (Ethylene Oxide): Benchmarks and Applications in Polymer Electrolyte. *Polymers* **2021**, *13*, 1131.
- (46) Wool, R. P. Polymer entanglements. *Macromolecules* **1993**, *26*, 1564–1569.
- (47) Molinari, N.; Mailoa, J. P.; Kozinsky, B. General Trend of a Negative Li Effective Charge in Ionic Liquid Electrolytes. *The Journal of Physical Chemistry Letters* **2019**, *10*, 2313–2319.
- (48) Yu, Z.; Balsara, N. P.; Borodin, O.; Gewirth, A. A.; Hahn, N. T.; Maginn, E. J.; Persson, K. A.; Srinivasan, V.; Toney, M. F.; Xu, K.; Zavadil, K. R.; Curtiss, L. A.; Cheng, L. Beyond Local Solvation Structure: Nanometric Aggregates in Battery Electrolytes and Their Effect on Electrolyte Properties. *ACS Energy Letters* **2022**, *7*, 461–470.
- (49) McEldrew, M.; Goodwin, Z. A. H.; Zhao, H.; Bazant, M. Z.; Kornyshev, A. A. Correlated Ion Transport and the Gel Phase in Room Temperature Ionic Liquids. *The Journal of Physical Chemistry B* **2021**, *125*, 2677–2689, PMID: 33689352.
- (50) Jones, S. D.; Bamford, J.; Fredrickson, G. H.; Segalman, R. A. Decoupling Ion Transport and Matrix Dynamics to Make High Performance Solid Polymer Electrolytes. *ACS polymers Au* **2022**, *2*, 430–448.
- (51) France-Lanord, A.; Grossman, J. C. Correlations from Ion Pairing and the Nernst-Einstein Equation. *Phys. Rev. Lett.* **2019**, *122*, 136001.
- (52) Shen, K.-H.; Hall, L. M. Ion Conductivity and Correlations in Model Salt-Doped Poly-

- mers: Effects of Interaction Strength and Concentration. *Macromolecules* **2020**, *53*, 3655–3668.
- (53) MacGlashan, G. S.; Andreev, Y. G.; Bruce, P. G. Establishment of the polymer electrolyte poly(ethylene oxide)6:LiAsF₆. *Nature* **1999**, *398*, 792–794.
- (54) Mao, G.; Saboungi, M.-L.; Price, D. L.; Armand, M. B.; Howells, W. S. Structure of Liquid PEO-LiTFSI Electrolyte. *Phys. Rev. Lett.* **2000**, *84*, 5536–5539.
- (55) Kang, P.; Wu, L.; Chen, D.; Su, Y.; Zhu, Y.; Lan, J.; Yang, X.; Sui, G. Dynamical Ion Association and Transport Properties in PEO–LiTFSI Electrolytes: Effect of Salt Concentration. *The Journal of Physical Chemistry B* **2022**, *126*, 4531–4542, PMID: 35695471.
- (56) Molinari, N.; Mailoa, J. P.; Kozinsky, B. Effect of Salt Concentration on Ion Clustering and Transport in Polymer Solid Electrolytes: A Molecular Dynamics Study of PEO–LiTFSI. *Chemistry of Materials* **2018**, *30*, 6298–6306.
- (57) Wheatle, B. K.; Keith, J. R.; Mogurampelly, S.; Lynd, N. A.; Ganesan, V. Influence of dielectric constant on ionic transport in polyether-based electrolytes. *ACS Macro Letters* **2017**, *6*, 1362–1367.

TOC Graphic

